International Journal of Heat and Mass Transfer 76 (2014) 286–297

Contents lists available at ScienceDirect

International Journal of Heat and Mass Transfer

journal homepage: www.elsevier.com/locate/ijhmt

Heat transfer mechanisms in isolated bubble boiling of water observed with MEMS sensor

Tomohide Yabuki [a,*], Osamu Nakabeppu [b]

[a] Department of Mechanical and Control Engineering, Kyushu Institute of Technology, 1-1 Sensui-cho, Tobata-ku, Kitakyushu, Fukuoka 804-8550, Japan
[b] Department of Mechanical Engineering, Meiji University, 1-1-1 Higashimita, Tama-ku, Kawasaki, Kanagawa 214-8571, Japan

ARTICLE INFO

Article history:
Received 16 July 2013
Received in revised form 3 April 2014
Accepted 4 April 2014
Available online 20 May 2014

Keywords:
Microlayer
MEMS
Nucleate boiling
Mechanism
Water
Microscale

ABSTRACT

Heat transfer characteristics of isolated bubble saturated pool boiling of water were investigated by local wall temperature measurement using an original micro-electro-mechanical systems (MEMS) sensor and a wall heat transfer evaluation. The measured temperature clearly indicated dynamic heat transfer phenomena below an isolated bubble including microlayer evaporation, dry-out of the microlayer, and rewetting of the dry-out region. Local heat removal due to microlayer evaporation exceeded 1 MW/m^2. Microlayer evaporation was found to have a central role in the wall heat transfer. The contribution of microlayer evaporation to bubble growth was about 50%, and did not vary significantly with wall superheat. The remaining 50% of the latent heat in the bubble was transferred from the superheated liquid surrounding the bubble. Finally, the spatial distribution of the initial microlayer thickness was calculated from the local heat flux of the wall.

1. Introduction

For more than half a century, several boiling heat transfer mechanisms have been proposed such as microlayer evaporation [1], contact line heat transfer [2], and evaporation of superheated liquid around a bubble [3] as latent heat transfer and convective heat transfer induced by bubble rising motion [4,5] and transient heat conduction within a liquid on the surface after bubble departure [6] as sensible heat transfer. Because conventional measurement techniques cannot precisely measure these elemental heat transfer phenomena that have very small temporal and spatial scales, quantitative verification of the proposed models has been insufficient. Therefore, aspects of the physical mechanisms of the nucleate boiling heat transfer remain unknown. On the other hand, the development of novel high resolution measurement techniques, e.g., micro-electro-mechanical systems (MEMS) sensors and high-speed infrared cameras permit detailed measurement of boiling heat transfer.

Demiray and Kim [7] and Myers et al. [8] used a micro heater array sensor with 96 heater elements with size $100 \times 100\ \mu m^2$ on a quarts or a silica substrate with heated area 1 mm^2 to measure the boiling of FC-72. Demiray and Kim conducted a boiling experiment under isothermal wall conditions, and the local wall heat transfer was evaluated from the feedback heating rate required to compensate for heat removal due to a single bubble boiling. Myers et al. evaluated the boiling heat transfer by heat conduction analysis using the measured temperature as the Dirichlet boundary condition. Both studies concluded that transient heat conduction is the dominant heat transfer mechanism, and the contribution of the latent heat transfer including the microlayer evaporation and the contact line heat transfer to the overall wall heat transfer is relatively small. Moghaddam and Kiger [9] developed a MEMS sensor with 44 platinum thin film resistance temperature detectors (RTDs) that were radially arranged on a silicon substrate where thin BCB (benzocyclobutene) layers with very low thermal conductivity were coated, and they measured the continuous bubble boiling of FC-72 under saturation conditions. They indicated that the transient heat conduction in the liquid thermal boundary layer that formed just after the passage of the advancing contact line was dominant at relatively low wall superheat, and micro-convection heat transfer became dominant at high wall superheat because of the shortened bubbling cycle. Contribution of microlayer evaporation and contact line heat transfer were indicated to be small as with Kim's group.

Wagner and Stephan [10] conducted micro-scale temperature measurements of FC-84, FC3284, and a binary mixture of them using a high-speed infrared camera, and demonstrated that high heat transfer occurred near a three-phase contact line during the advancing and receding processes. However, they indicated that the contribution of the three-phase contact line heat transfer to

* Corresponding author. Tel.: +81 93 884 3138.
E-mail address: yabuki@mech.kyutech.ac.jp (T. Yabuki).

http://dx.doi.org/10.1016/j.ijheatmasstransfer.2014.04.012
0017-9310/

Nomenclature

D_{max}	maximum bubble diameter [m]
h_{lv}	latent heat of vaporization [J/kg]
$\dot{q}$	local heat flux [W/m^2]
$\dot{q}_b$	base heat flux [W/m^2]
Q_b	latent heat in bubble [J]
Q_{ml}	microlayer heat [J]
Q_{sl}	liquid phase heat [J]
Q_w	heat transferred from heating surface [J]
$\dot{Q}_b$	bubble growth rate [W]
$\dot{Q}_{ml}$	heat flow transferred by microlayer evaporation [W]
$\dot{Q}_{sl}$	heat flow transferred by evaporation of superheated liquid layer [W]
$\dot{Q}_w$	Wall heat flow [W]
r	radial position [m]
R_b	bubble radius [m]
R_c	radius of apparent contact area [m]
R_{eq}	equivalent bubble radius [m]
$R_{dry\text{-}out}$	radius of dry-out region [m]
R_{max}	maximum bubble radius [m]
R_{ml}	radius of microlayer region [m]
t	time [s]
t_{dp}	time at bubble departure [s]
t_{nc}	time at bubble nucleation [s]
t_{me}	duration of microlayer evaporation [s]
T_r	temperature at reference junction [°C]
T_s	temperature at sensing junction [°C]
V_{TC}	bubble volume [m^3]
V_{TC}	electromotive force [V]
α	thermoelectric power [V/K]
δ	amount of evaporated microlayer [m]
δ_0	initial microlayer thickness [m]
ΔT_{sat}	wall superheat [K]
ΔT_{sub}	liquid subcooling [K]
ρ_l	density [kg/m^3]

the overall wall heat transfer was small. Using a high-speed IR camera, Gerardi et al. [11] showed that the largest enthalpy required for bubble growth is transferred by microlayer evaporation during the saturated boiling of water.

Based on recent advancements in computational fluid dynamics (CFD) techniques and computer technologies, numerical studies that accurately solve governing equations and apply superior interface tracking methods have been actively conducted to elucidate physical mechanisms of the boiling phenomena [12,13]. The micro-scale temperature and heat transfer data measured with the MEMS sensors and the high-speed cameras are considered useful for validating the numerical simulation results.

Table 1 shows a comparison of the spatiotemporal resolutions of the MEMS sensor and the high-speed IR camera used in the boiling studies. There is little difference in the spatial resolutions of the MEMS sensor and the high-speed IR camera. The IR camera can measure the surface temperature of a relatively wide area, and hence, no artificial nucleation site is required. Therefore, the IR camera can be applied to the high heat flux experiments for events such as triggering mechanisms for CHF (critical heat flux). Although the MEMS sensor is restricted in that bubbles have to be generated from predetermined positions, it is superior to the IR camera in terms of its temporal resolution. By reducing the sensor size and film thickness, an extremely high spatiotemporal resolution can be realized.

Fig. 1 shows a schematic of heat transfer paths in the isolated bubble saturated boiling of water and the findings of this study include the contribution of the microlayer evaporation to the bubble growth, local heat flux, and the spatial distribution of the initial microlayer thickness. Because the contribution of the transient heat conduction to the overall wall heat transfer was small, and the present study did not indicate any significant effect of Marangoni convection along the bubble surface, the heat transfer paths taken by these two mechanisms were not indicated in Fig. 1. To simplify the problem, the effects of the interaction between bubbles, bubble condensation due to liquid subcooling, bubble nucleation, and bulk liquid flow were removed from this study. In the non-boiling condition or the waiting period during $t < t_{nc}$, the heat supplied from the heat source was transferred to bulk fluid by heat conduction within the heating wall and the liquid thermal boundary layer, and by natural convection in the liquid phase. Forced convection is expected to occur after the departure of the bubble. In the heat transfer paths arising under the boiling condition, the latent heat in the bubble Q_b is supplied by the evaporation of the

Table 1
Comparison of spatiotemporal resolutions of MEMS sensor and high-speed infrared camera.

Measurement method	Research group	Spatial resolution	Temporal resolution (data acquisition rate)
MEMS	Kim [7]	100 μm	3704 Hz
MEMS	Moghaddam [9]	22–40 μm	8 kHz
MEMS	Present study	20 μm	50 kHz
IR camera	Stephan [10]	14.5 μm	978 Hz
IR camera	Buongiorno [11]	100 μm	500 Hz
IR camera	Kenning [14]	40 μm	1 kHz

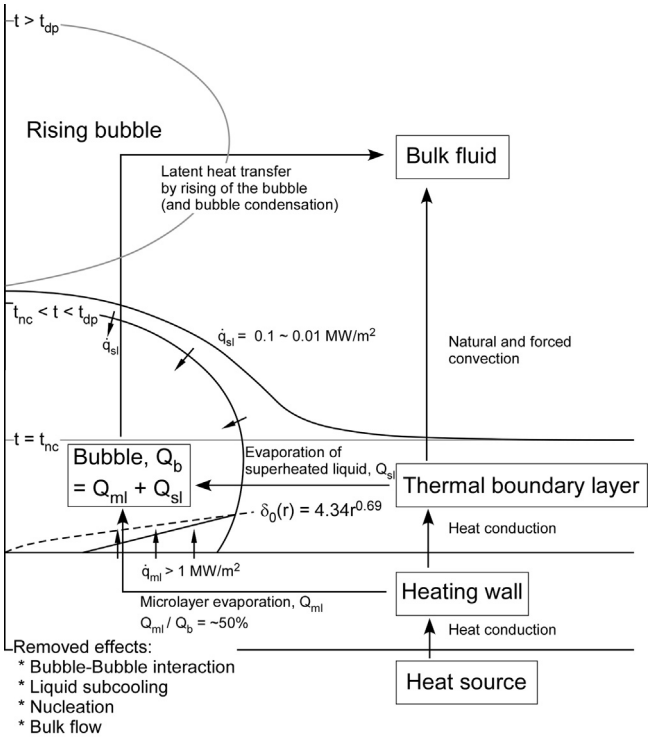

Fig. 1. Schematic of heat transfer paths in water pool saturated boiling and findings of this study.